JOURNAL OF GEOPHYSICAL RESEARCH, VOL. 111, C12013, doi:10.1029/2006JC003578, 2006

A comparison of sea surface temperatures from microwave remote sensing of the Labrador Sea with in situ measurements and model simulations

William J. Emery,[1] Peter Brandt,[2] Andreas Funk,[2] and Claus Böning[2]

Received 16 March 2006; revised 28 June 2006; accepted 17 July 2006; published 15 December 2006.

[1] As one of the few places in the ocean where winter cooling and mixing creates conditions where water from the surface can penetrate into the deep ocean the Labrador Sea is an area of interest to people studying climate change in the ocean. Persistent cloud cover over this area makes it impossible to use infrared satellite imagery to relate space/time changes in sea surface temperature (SST) to changes in surface currents and air-sea interaction. Using passive microwave SSTs from the Advanced Microwave Scanning Radiometer (AMSR-E), we plot space/time changes in SST in the Labrador Sea and relate these changes to both simultaneous in situ measurements of temperature and numerical model SSTs. A direct comparison between the microwave SSTs, infrared SSTs, and in situ temperatures measured from profiling floats reveals that the microwave SSTs are a good representation of space/time changes in infrared SST and in ocean temperatures down to 10 m below the sea surface. Comparisons between the microwave SSTs and time series of temperatures at depths below 50 m reveal that winter/spring surface cooling makes the SST similar to temperatures at these deeper depths in the convection region of the central Labrador Sea. Detailed comparison of the annual cycle between the microwave SSTs and the model SST and 10 m currents reveals overall good agreement and some interesting differences.

Citation: Emery, W. J., P. Brandt, A. Funk, and C. Böning (2006), A comparison of sea surface temperatures from microwave remote sensing of the Labrador Sea with in situ measurements and model simulations, *J. Geophys. Res.*, *111*, C12013, doi:10.1029/2006JC003578.

1. Introduction

[2] The Labrador Sea is one of a very few regions where the ocean regularly forms vertical columns of neutral density where surface waters can easily penetrate down into the water column [*Marshall and Schott*, 1999; *Lazier et al.*, 2002; *Stramma et al.*, 2004]. The local eddy field is thought to play an important role in preconditioning this vertical exchange as well as in the restratification of the Labrador Sea after the convective period [*Prater*, 2002; *Lilly et al.*, 2003; J. Chanut et al. (2006), Mesoscale eddies in the Labrador Sea and their contribution to convection and restratification, submitted to *Journal of Physical Oceanography,* 2006, hereinafter referred to as Chanut et al., submitted manuscript, 2006]. Unfortunately persistent cloud cover over the Labrador and Greenland Sea regions makes it difficult to use infrared satellite SST measurement techniques to observe the surface layer cooling that gives rise to the onset of these vertical exchange events.

[3] An example of the difficulty in using satellite infrared temperatures of the study region is presented here in Figure 1, which shows weekly SSTs from January and June, 2003 as computed from the NASA Pathfinder SST product available at NASA's Jet Propulsion Laboratory. They are based on the 11 and 12 μm channels of the advanced very high resolution radiometer (AVHRR) computed from the 4 km resolution Global Area Coverage (GAC). In these images the white areas represent regions where no SSTs can be retrieved due to persistent cloud cover. The cold SSTs of the study region are suggested by the patches of light and dark blue in the maps with the occasional green area. The corresponding temperatures are given in the color scales showing that the surface temperatures in this region range between the freezing point and 4 °C in winter.

[4] Even in the summer month of June 2003 (Figure 1, bottom) it is difficult to clearly see the SST patterns in the Labrador Sea due to cloud obscuration. There is evidently more clear sky as demonstrated by the increase in color segments of these SST maps but these colors do not dominate the entire study region and the breaks in the colored regions are enough to disrupt the picture of SST changes in space and time. Only in the first week of June one can see a somewhat coherent spatial pattern of infrared SST. SST now ranges from temperatures near the freezing point in the north to about 10°C in the south. One still cannot see the details of the

[1]Department of Aerospace Engineering Sciences, University of Colorado, Boulder, Colorado, USA.
[2]Leibniz-Institut für Meereswissenschaften an der Universität Kiel, Kiel, Germany.

0148-0227/06/2006JC003578$09.00

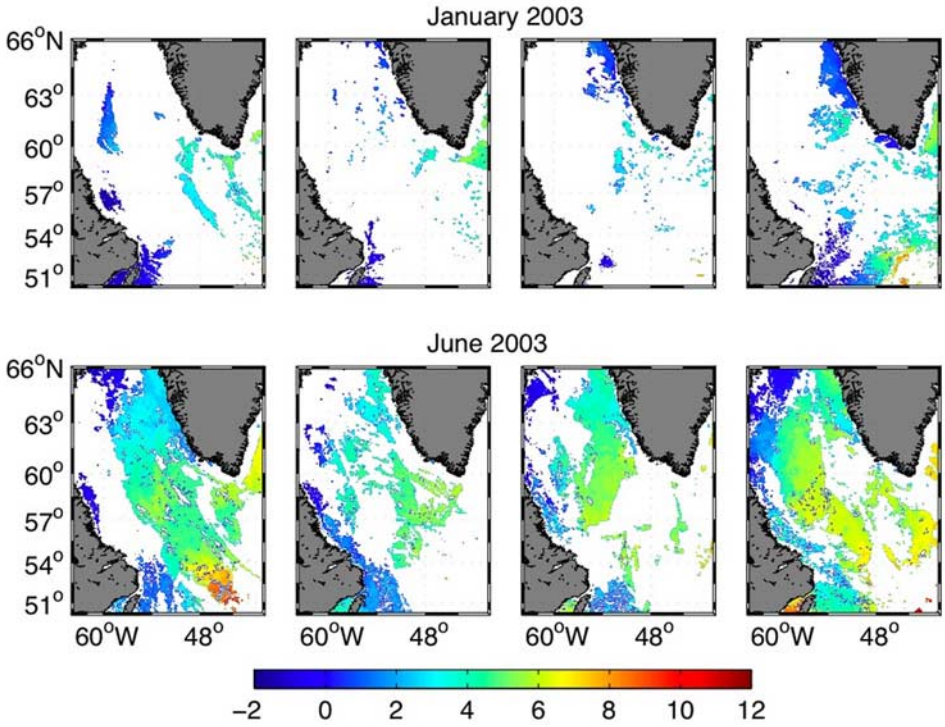

Figure 1. Weekly thermal infrared images of sea surface temperature in °C from NASA's Pathfinder Project.

SST in the northern region, which is known to be populated with mesoscale eddies and meanders [*Prater*, 2002].

[5] In contrast the same presentation for AMSR-E microwave SST in Figure 2 shows a continuous presentation of SST for both January and June of 2003. The major limitation in these SST maps is the fact that the microwave SSTs are excluded from consideration close to the shoreline where contamination of the large microwave spots (~50 km) is

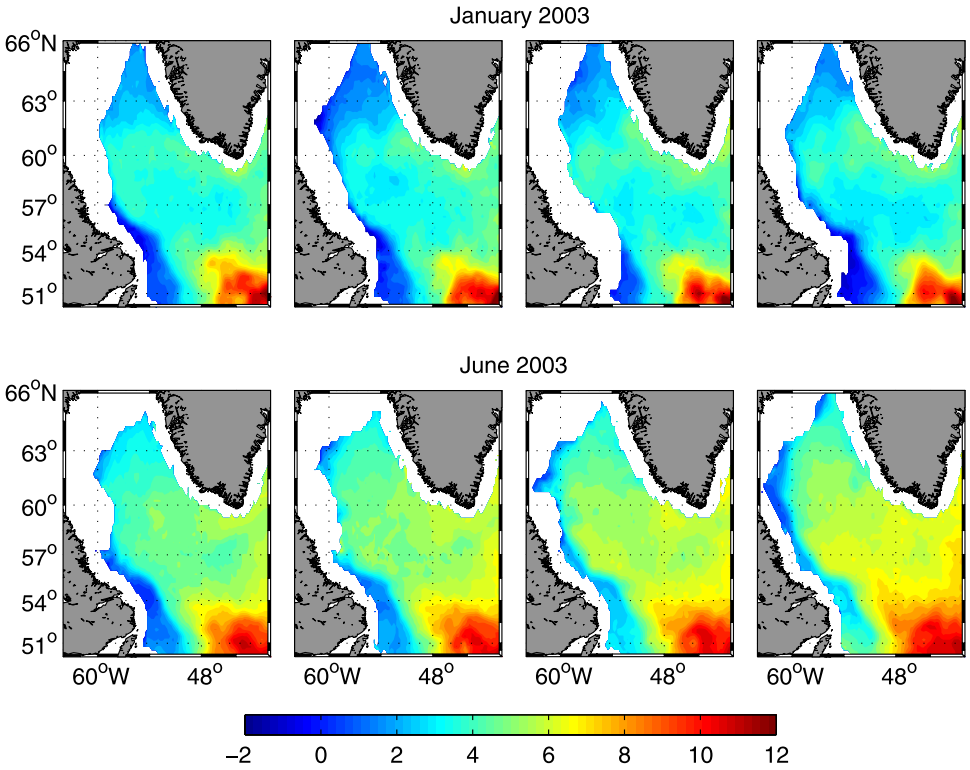

Figure 2. Weekly AMSR-E passive microwave SST in °C.

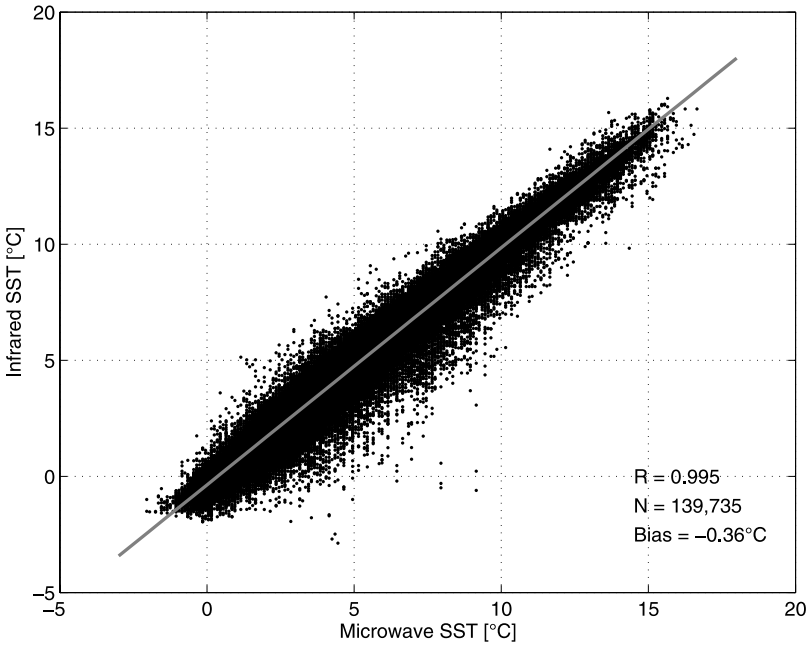

Figure 3. Regression of infrared SST on AMSR-E passive microwave SST.

likely. Additionally regions are marked out where AMSR-E microwave SSTs are contaminated by ice coverage resulting in a band of white along the coastline.

[6] A conspicuous feature in Figure 2 is the emergence of a band of warmer waters in January extending from the east toward the west across the central Labrador Sea at about 60°N. This is most clearly marked in January in Figure 2 as a band of green surrounded by lighter blue (colder) water to the north and south. This feature is either absent or only very weakly developed in the June summer images (Figure 2) and it could not be seen in the infrared images at all. The annual cycle of AMSR-E microwave SST will be discussed later when the Hovmoeller plots of AMSR-E microwave and numerical model SST will be presented. A similar analysis of the infrared images (not presented) demonstrated that it would be almost impossible to characterize the annual variations of the SST from the infrared images.

2. Statistical Comparison Between Infrared and Microwave SST

[7] The Advanced Microwave Scanning Radiometer for EOS (AMSR-E) is a Japanese built total power microwave radiometer with channels between 6.9 and 89 GHz. A conical scanning instrument it has a spatial resolution of 56 km for the 6.9 GHz channel that is optimal for measuring SST. At this frequency the sensitivity is given as 0.3 K for an integration time of 2.6 ms. AMSR-E is carried by NASA's Aqua satellite, which was launched on 4 May 2002 into the afternoon Sun synchronous orbit now known as the A-Train.

[8] Remote Sensing Systems (RSS) computed the AMSR-E SST retrievals used in this study as part of their NASA funded data system activity. In the generation of their microwave products RSS carries out quality checks to detect AMSR-E cells affected by rain or undetected sea ice. In this study comparisons are carried out with in situ SST measurements and with other infrared satellite SSTs. An SST match up data set was created between weekly AVHRR infrared and AMSR-E microwave SSTs by extracting microwave SST when the infrared image was found to be cloud free and the microwave SST was beyond the coastal contamination. These match ups covered the period June 2002 through September 2004.

[9] A regression of the infrared SST against the microwave SST (Figure 3) yielded a correlation of R = 0.995 with a bias of −0.36°C for a sample size of 139,735. This bias indicates a cooler infrared SST consistent with the "skin effect" in spite of the fact that the NASA Pathfinder infrared SST is regressed on buoy SSTs converting the infrared satellite "skin" radiances into a "quasi-bulk SST."

[10] As can be seen in Figure 3, there is some indication that the negative bias is greater at low temperatures which would suggest that the skin effect is larger in winter than in summer when surface heating causes vertical stratification including the few centimeters below the surface that the AMSR-E microwave SST represents.

[11] Separating the data into summer and winter data and repeating the regression confirmed this. The summer result is presented here in Figure 4, which has a correlation of 0.996, a bias of −0.18°C and a total sample size of 85,621. The winter bias was −0.46°C, the correlation of 0.990 and a sample size of 54,114 (Figure 5). Thus, in the winter when the water column becomes vertically homogeneous and convection occurs the skin-bulk SST difference is at a maximum while in the summer when solar heating stratifies the upper layer this difference decreases. This increased skin-bulk difference in winter might reflect the stronger winter winds and higher outgoing heat flux from the ocean. At the same time, however, higher winds increase upper layer turbulence and leads to capillary wave breaking which makes the skin-bulk temperature difference smaller. It should be noted, however, that there is a strong summer sampling bias with more than 85,600 match ups in summer and just over 54,000 match ups in winter.

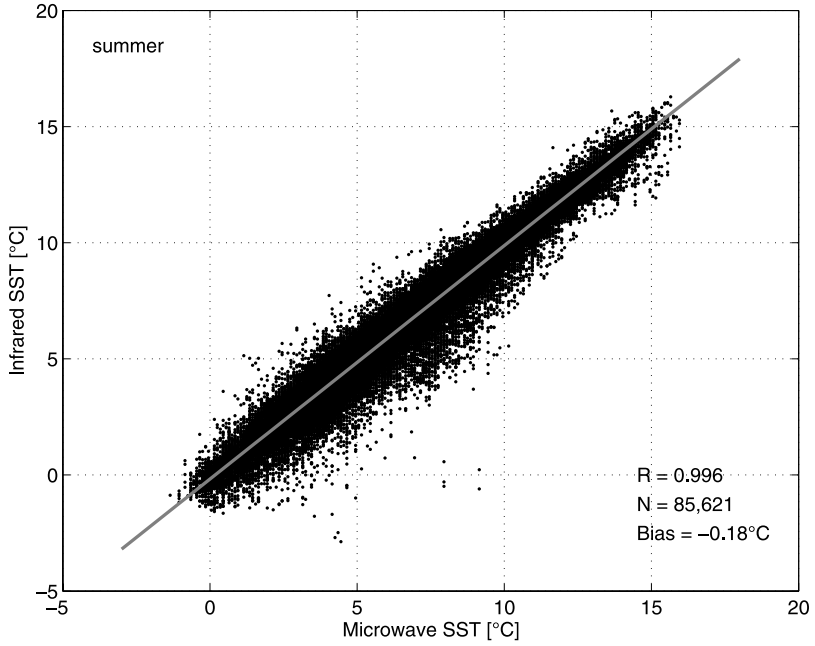

Figure 4. Regression of infrared SST on AMSR-E passive microwave SST in summer.

[12] Again as in the overall regression the low temperatures appear to have a greater negative bias (infrared is cooler) than is seen at the higher temperatures. The sampling bias toward summer is clearly reflected in the 34 % more temperature match ups found in summer compared to winter. This confirms statistically what we could see in Figure 1 that the winter infrared images were so poorly represented that they could not be used to define the SST field.

3. Comparison With in Situ Temperatures

[13] For the period June 2002 through September 2004 we compared the AMSR-E microwave SSTs with the nearest to the surface temperatures measured by the autonomous ARGO floats in our study region. The positions of all the ARGO float observations from 2002 to 2004 are presented here in Figure 6. The majority of the floats are in 2003 (blue) and 2004 (red) with fewer points in 2002. This plot also shows the locations of two moorings in the central and southern Labrador Sea with data that will be compared with the AMSR-E microwave SSTs. We cut off the ARGO float data at the end of 2004 as this comparison study was carried out in 2005 and the in situ data were available only for the earlier years.

[14] We extracted all of the AMSR-E microwave SSTs to match the locations and times of the ARGO float upper temperature data. The uppermost temperature measurement

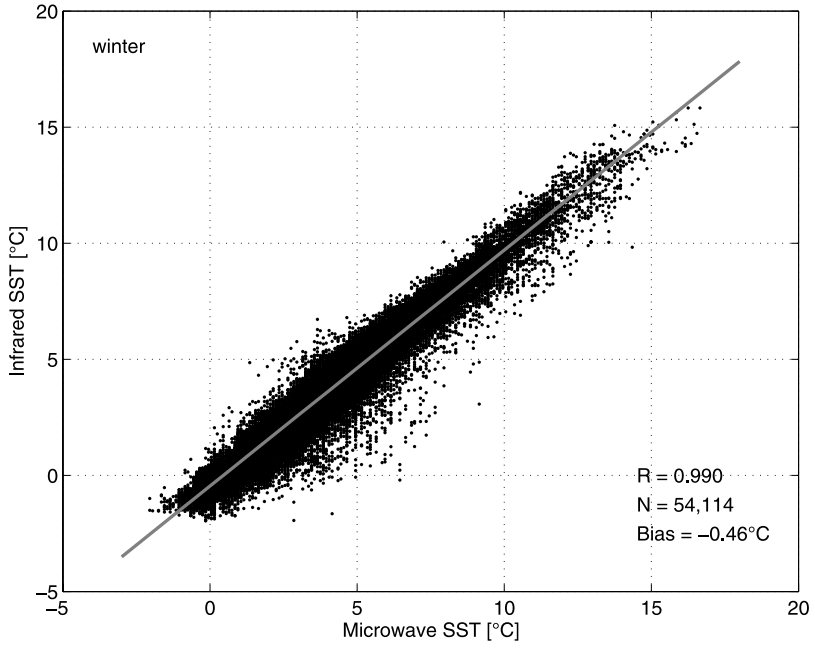

Figure 5. Regression of infrared SST on AMSR-E passive microwave SST in winter.

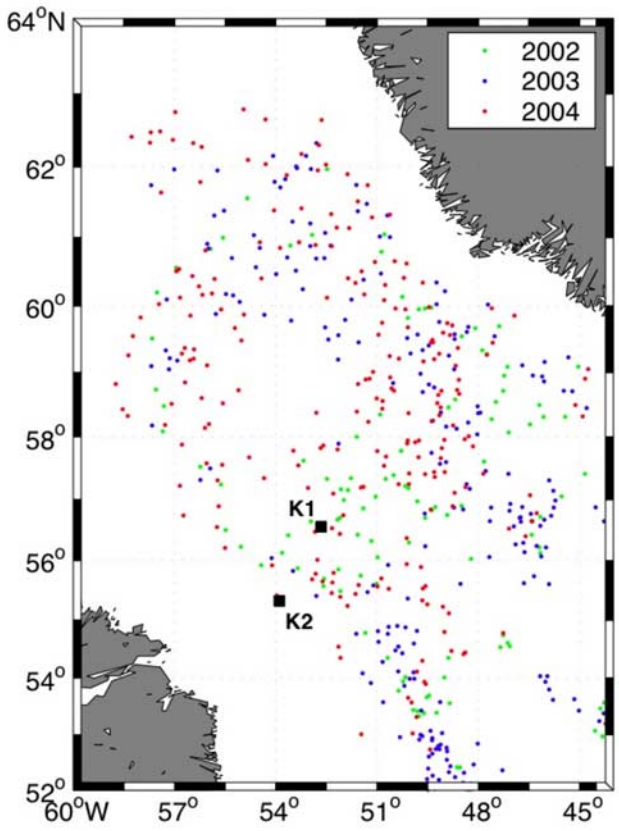

Figure 6. Positions in the Labrador Sea of all the ARGO float observations 2002–2004.

is typically taken at a depth of about 5–10 m at the end of each profile. During their surface drift needed to transfer acquired data to a satellite no temperature/salinity measurements are performed.

[15] Plotting the microwave SST against the float temperatures (Figure 7) we found a surprisingly good agreement between the two. A regression line (red) was fit to the scatter points which gave a correlation of R = 0.997 which is 99% significant for the N = 570 data values. We again note that there is a slight bias toward summer measurements as there were fewer match ups between microwave SSTs and float temperatures in winter.

[16] The almost zero bias of −0.04°C demonstrates that the float temperatures were in general very similar to the microwave SSTs which was a surprise since the float data generally represent subsurface (∼10 m) temperatures. The positive relationship between the microwave SSTs and the ARGO float upper layer temperatures strongly suggests that we should be able to see upper layer ocean processes in the space/time changes of the microwave SSTs. This will be further evident when we compare model circulation features with the AMSR-E SSTs.

[17] At two mooring locations in the central Labrador Sea (K1) and in the deep Labrador Current near Hamilton Bank (K2) we plot time series of AMSR-E microwave SST with the shallowest temperatures from the moorings, which were at 73 and 97 m depth respectively (Figure 8). Unfortunately the moored record only covers the first year. Still the comparison over this short period exhibits some very interesting features. While mooring K1 is representative of the central Labrador Sea regime with deep mixed layer depths during winter, mooring K2 represents the Labrador Current regime.

[18] During the late fall, winter and spring months the AMSR-E microwave SST is very similar in magnitude to the deeper temperatures at mooring position K1 suggesting vertically homogeneous conditions in the region prevail in the upper 100 m consistent with vertical mixing processes. It should be noted that K1 is located in the deep convection region of the central Labrador Sea [*Lavender et al.*, 2000]

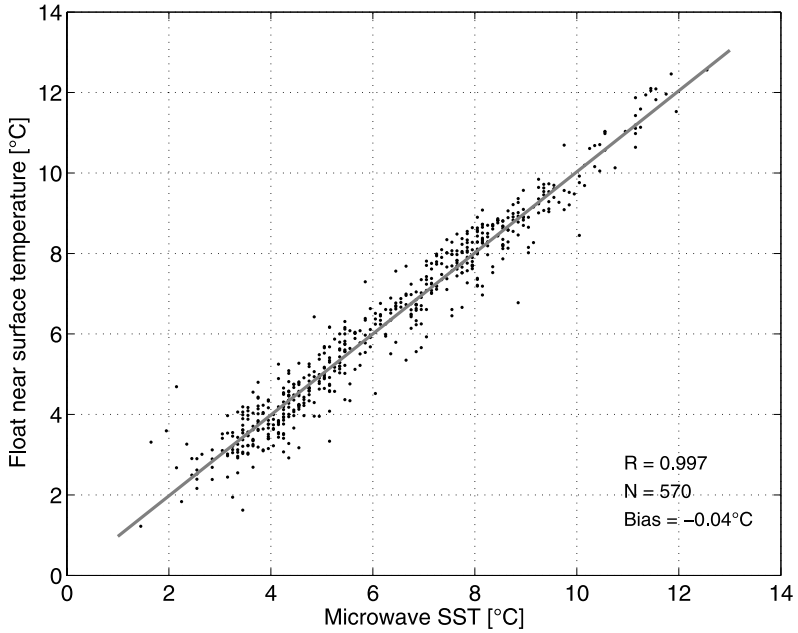

Figure 7. Relationship between AMSR-E passive microwave SST and ARGO float near-surface temperatures.

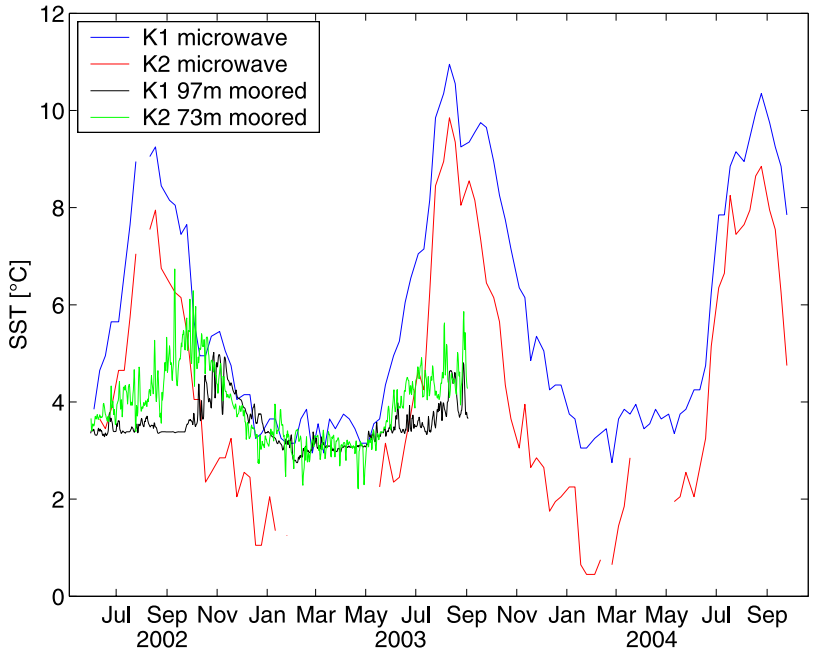

Figure 8. Time series of AMSR-E passive microwave SST (red/blue) and deeper moored temperatures (green/black) at two positions near Hamilton Bank (see Figure 6).

while K2 is not. From May to early fall near surface heating warms the centimeter deep AMSR-E microwave SST dramatically as compared with the deeper temperatures. This surface heating is associated with a shallow seasonal thermocline and causes the SST time series to peak in August while the deeper temperatures reach their maximum value in fall where the two time series curves tend to come together again.

[19] At mooring position K2 such behavior cannot be observed. While during summer the AMSR-E microwave SSTs are larger than deeper temperatures, during the rest of the year they are smaller indicating the presence of a cold and fresh surface layer at the top of the deep Labrador Current during most of the year. While this layer is colder its low salinity stabilizes it and it stays on the top. The observed difference between microwave SST and moored subsurface temperature at the mooring position K2 suggest that convection associated with vertical mixing down to the uppermost temperature sensor of the mooring (97 m) does not occur at this position. However, there is a gap in the microwave data from February to May 2003 possibly due to ice coverage. In 2004, the wintertime gap is smaller showing an increase in the microwave temperature during March. This increase in the microwave SST that cannot be associated with surface heat fluxes may be associated with the upward mixing of heat from the subsurface temperature maximum toward the sea surface.

4. Comparison With Model SSTs

[20] To elucidate the AMSR-E microwave SST variations they are compared with results from an eddy-resolving model that is part of FLAME (Family of Linked Atlantic Model Experiments) and uses a horizontal grid of 1/12° in longitude, which corresponds to a mesh size of about 5–6 km in the Labrador Sea. The model has been used by *Eden and Böning* [2002] to study eddy generation in the Labrador Sea. For the model run analyzed here a refined configuration for the subpolar North Atlantic developed by *Czeschel* [2004] was adopted, which includes an isopycnal scheme for subgrid-scale diffusion (with a diffusivity of 50 m^2/s), and a biharmonic viscosity (with a friction coefficient of 2×10^{10} m^4/s). The model run is the same as by *Brandt et al.* [2006] driven by a climatological forcing with monthly mean fields of the years 1986–1988. The model mean SST is compared with the 2-year mean AMSR-E microwave SST in Figure 9. We overlaid the model 10 m currents on the model mean SST to better understand the role of the model currents in creating the distribution of the observed SST. In the AMSR-E microwave SST the land and ice contamination boundary unfortunately eliminates some of the detailed features of the model SST. Still the general agreement is quite good with similar warm waters in the region of the Northwest Corner of the North Atlantic Current intruding into the Labrador Sea at the southwest, adjacent to cooler water in the central Labrador Sea. While the coldest SSTs of the model simulations are found in the Northwest and along the shallow boundary currents over the shelves, microwave SSTs show similar cold temperatures only north off Greenland as the coastal regions are eliminated.

[21] The band of warm SST crossing the whole Labrador Sea at about 59°N that was discussed already for the January microwave SSTs (Figure 2), is also evident in the mean AMSR-E microwave SST image. However, it is much weaker in the model results extending only slightly from the eastern boundary toward west. The annual mean 10 m currents suggest the existence of a couple of zonal bands that flow from eastern boundary to the west. The AMSR-E microwave SSTs with their poor spatial resolution are unable to properly capture the abundance of mesoscale

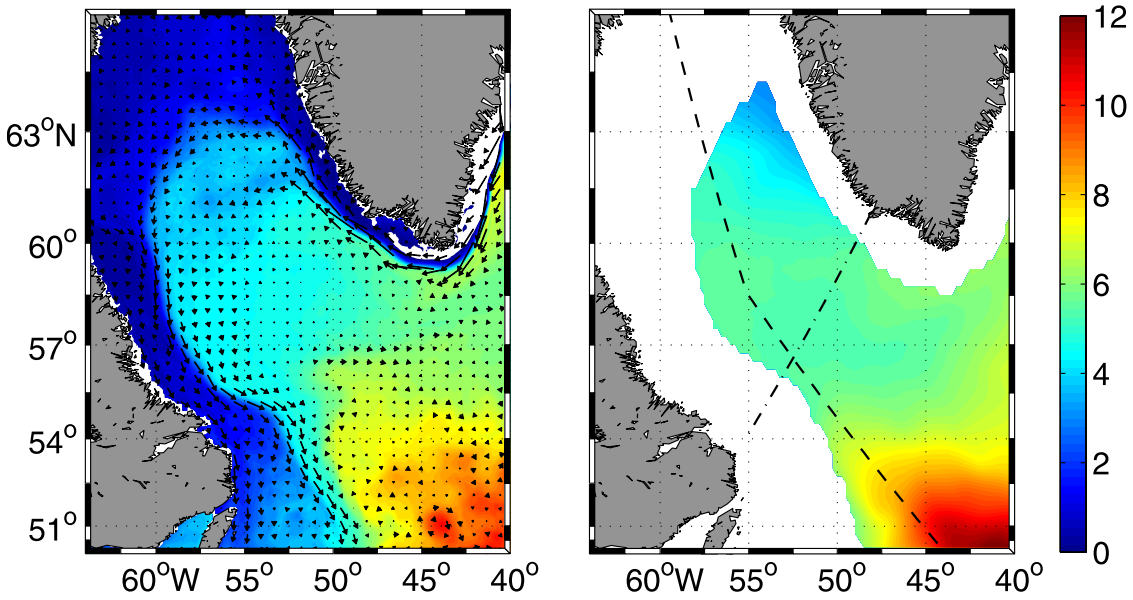

Figure 9. (left) Annual mean model SST overlaid on 10 m currents and (right) 2-year mean AMSR-E microwave SST. Temperatures are given in °C. The dashed and dashed-dotted lines in Figure 9 (right) mark the sections along the axis of the Labrador Sea and the WOCE AR7W section, respectively.

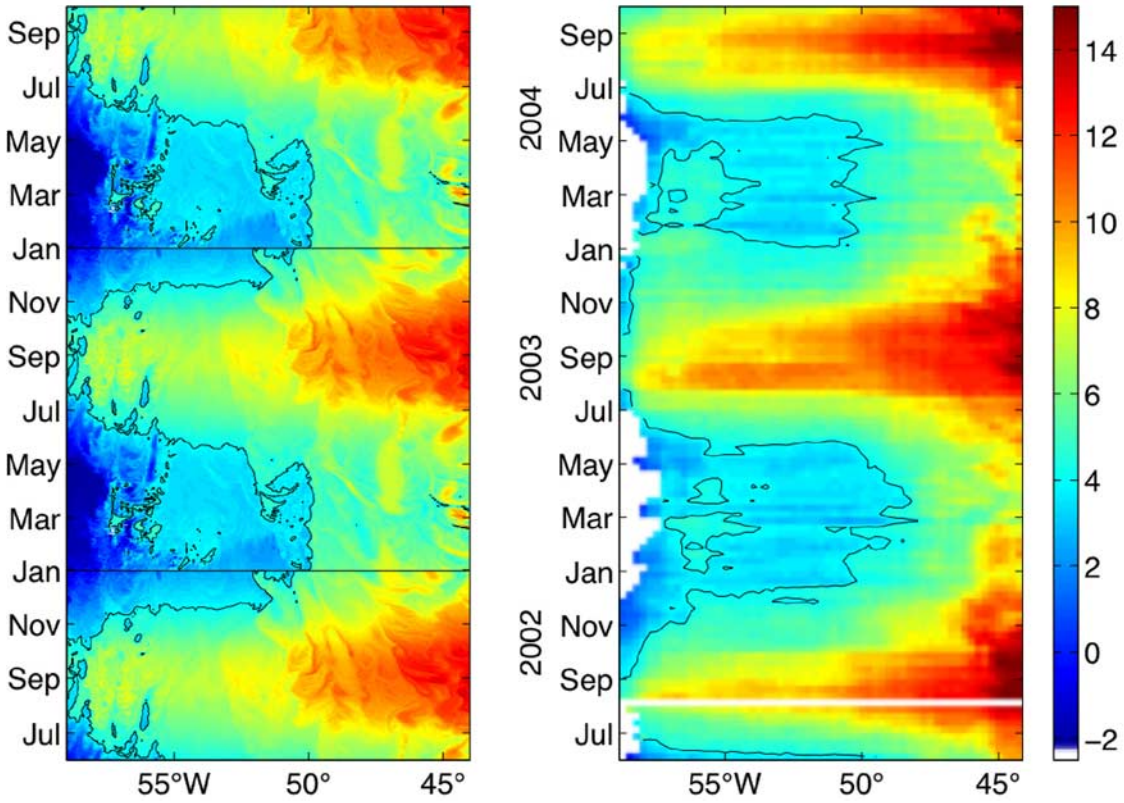

Figure 10. Hovmueller diagram of SST in °C along the dashed line in Figure 9, (left) from the numerical model (repeated annual cycle) and (right) from AMSR-E. The solid dark line indicates the 4 °C isotherm.

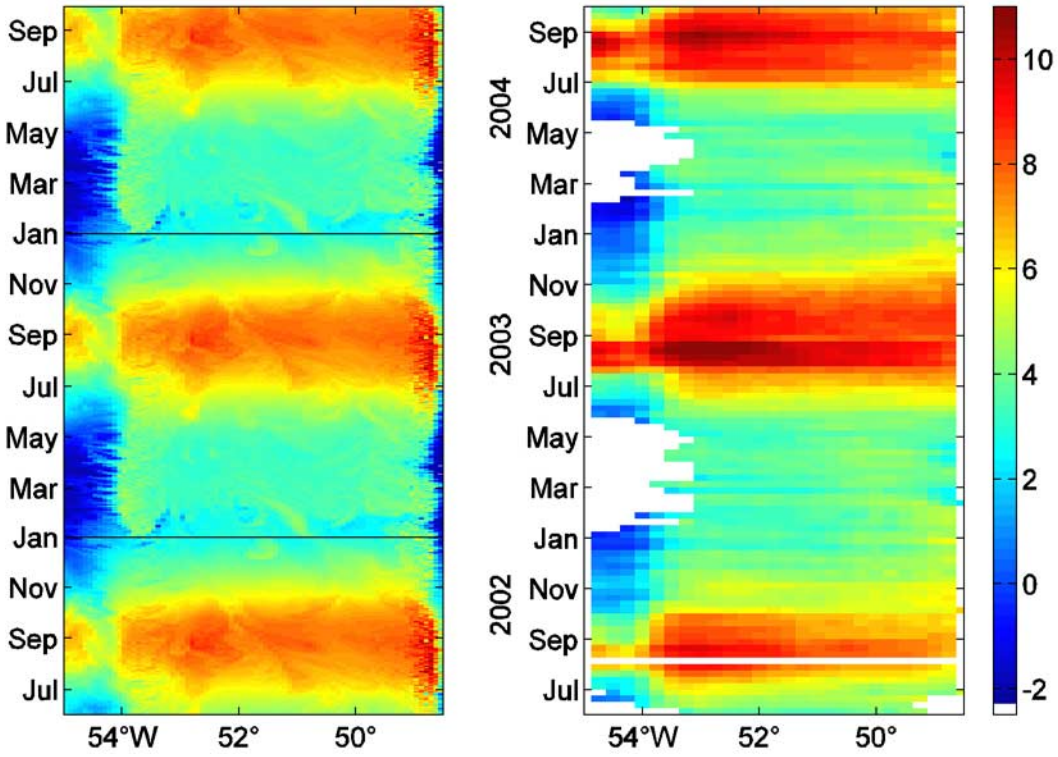

Figure 11. Hovmueller diagram of SST in °C along the AR7W section (see dash-dotted line in Figure 9), (left) from the numerical model (repeated annual cycle) and (right) from AMSR-E.

eddies present in this region that are indicated by the mean model output. It should be pointed out that the ~ 50 km spatial footprint of AMSR-E is much larger than the <10 km internal Rossby radius in the Labrador Sea. As mentioned earlier these eddies contribute significantly to the preconditioning of convection and restratification after the convection in the Labrador Sea (Chanut et al., submitted manuscript, 2006).

[22] The general correspondence between the model and microwave SSTs is more apparent in the Hovmoeller diagram shown in Figure 10. Here the model SST annual cycle has been repeated on the left for comparison with the time series of microwave SST. The distances along the x axis of this plot are taken along the axis of the Labrador Sea as shown in Figure 9. In general there is a good agreement between model and microwave SST space/time changes. Most pronounced in both fields is the seasonal warming with highest temperatures in August. Between January and May temperatures below 4°C mark the central Labrador Sea. In the AMSR-E microwave SST this patch of cold temperatures is separated by a band of warmer water from the coldest temperatures in the Northwest. A possible explanation for the band of warmer temperatures is that it is generated during winter when warmer and saltier water masses that are transported at intermediate depths off the shallow West Greenland Current into the Labrador Sea [*Cuny et al.*, 2002] are mixed in the near boundary current regime toward the surface. As revealed by the AMSR-E microwave SSTs the band of local temperature maximum north of the convection region is more pronounced during winter 2004 than winter 2003. Strong year-to-year variability is also found south of the convection region. While during March 2003 cold temperatures reach as far as 48°W, during March 2004 cold SSTs are blocked at about 50°W. Here warmer waters are possibly intruding from the southeast.

[23] In contrast to the observations the band of warm temperatures north of the main convection region does not appear to be present in the repeat annual cycle of the numerical model. Moreover the model results suggest during December/January cold temperatures intruding from the North into the central Labrador Sea. This temperature minimum in the model is associated with the shedding of mostly anticyclonic eddies from the West Greenland Current into the central Labrador Sea [*Eden and Böning*, 2002]. These eddies are generally composed of a shallow fresh and cold surface layer [*Lilly et al.*, 2003]. Although good agreement between observed and simulated location and annual cycle of West Greenland Current eddy generation was found using similar model results and altimetric observations [*Eden and Böning*, 2002; *Brandt et al.*, 2004], the model seems to overestimate the transport of cold and fresh surface waters along the migration pathway of West Greenland Current eddies into the central Labrador Sea.

[24] Summer 2003 appears to be anomalous in the occurrence of the warm surface temperatures in the central Labrador Sea. In mid-2003 two very distinct peaks with the first occurring in August and the second in October can be observed. None of the other two summers has two distinctly different peaks. Earlier 2002 there is a much weaker first

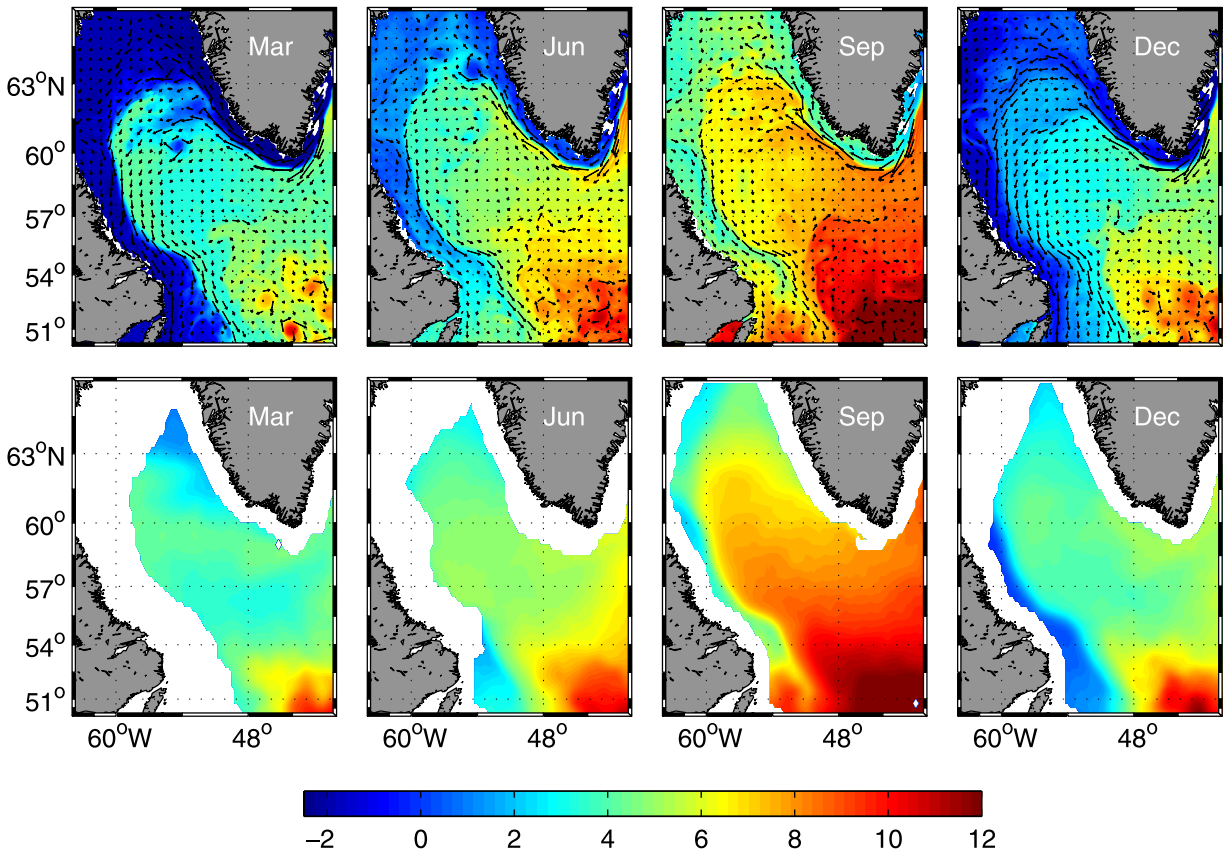

Figure 12. (top) Monthly mean model SST and 10 m current and (bottom) monthly mean AMSR-E SST. Temperatures are given in °C.

peak with a broadening of the subsequent peak, which does not extend as far north as that in 2003. Taken across a section at the central Labrador Sea (WOCE AR7W section) the Hovmoeller diagram in Figure 11 shows again in general a good agreement between model and microwave SSTs in the structure of the mean seasonal cycle. However, it gives a slightly different view of the temporal variations in Figure 10. While during summer 2003 largest microwave SSTs are observed lasting from July to November in the central and northeastern part of that section, during summer 2002 the microwave SSTs are smaller and significant cooling can be observed as early as October. In the region of the shallow Labrador Current, the period of warm SSTs is much shorter compared to the central part of the section (Figure 11). Here microwave SSTs reveal maximum temperatures in August with longest duration of warm temperatures in 2004 and weakest temperature maximum in 2002. The interannual variations of AMSR-E microwave SST may be attributed both to variations in air-sea forcing and to changes in the local ocean circulation.

5. Annual Time Series Comparison

[25] To get a more detailed understanding of the space/time changes of the SST and 10 m currents in the Labrador Sea we compared monthly mean SSTs from the model and AMSR-E along with the monthly mean model 10 m currents. The corresponding fields are presented here for the four months (March, June, September, December) in Figure 12. This time series clearly shows the differences and similarities of the microwave and model SSTs. The higher spatial resolution of the model SSTs clearly depicts the mesoscale eddy field that dominates in the warm southern portion as well as in the cold northern portion of the Labrador Sea particularly in March. In the lower-resolution AMSR-E microwave SSTs the eddies are expressed only by meanders in the warm SSTs. Moreover, the small intrusion of cold surface waters advected along the shallow Labrador Current that are clearly visible in the September model field are only poorly resolved in the AMSR-E microwave fields.

[26] During December, the central Labrador Sea SSTs are warmer in the AMSR-E microwave data when compared with the model fields. Particularly warm SSTs can be observed in the AMSR-E microwave data north of the central Labrador Sea during December and March that are extending as a band of warm water from east to west. In the model, this band is completely missing in December, while in March warmer SSTs are found in the northwestern part of the Labrador Sea. In the model, the reason for the increase of SSTs from December to March in the western part of the deep Labrador Sea is the advection of warm subsurface waters along the cyclonic Labrador Sea boundary current and subsequently vertical mixing. However, the model shows much colder SSTs particularly in the West Greenland Current eddy shedding region compared with the microwave SSTs. This could result from the fact that the model overestimates the advection of cold surface temperatures along the eddy migration pathway. Although the March

microwave SSTs also reveal the existence of a cold tongue extending from the eastern boundary into the central Labrador Sea, it does not interrupt the band of warm SSTs at about 59°N separating the cold temperatures in the central Labrador Sea from even colder SSTs farther north.

[27] By June SSTs have warmed up to about 6 °C in both the model and AMSR-E microwave fields for the central Labrador Sea. Here the model field shows a narrow extension of the Irminger Current marked by warm SSTs in the northern Labrador Sea that is not present in the microwave SST monthly maps. In September both fields show a northward extension of the warm SSTs but the microwave SSTs display a broader intrusion into the Labrador Sea shifted toward the south, while the model SSTs restrict the warmest waters to a northward extension along the northeastern boundary current. In the model, a northward surface flow at about 50°W away from the southern boundary current accounts for the lack of an inflow of warmer surface waters into the western part of the Labrador Sea. Microwave SSTs on the other side suggest the existence of a recirculation off the deep Labrador Current that allows warmer surface waters to be advected into the southwestern part of the Labrador Sea. During December the narrow warm tongue found in the summer model SSTs has vanished, as have any remnants of the AMSR-E warm SST intrusions in the southern portions of the Labrador Sea.

6. Conclusion and Discussion

[28] SSTs computed from the 6.9 GHz channel on AMSR-E are used to map space/time changes in SST in the Labrador Sea. Similar maps made from coincident infrared satellite imagery are clearly inadequate to view the changes revealed by the AMSR-E imagery due to persistent cloud cover in the region. Infrared SSTs are, however, found to correlate well with the AMSR-E SST when both are present. A negative bias of about −0.36 °C is found indicating cooler infrared SSTs consistent with the fact that the microwave measure temperatures slightly deeper (∼1 cm) than the 10 micron thin infrared SST emissions. The microwave SST changes are found to correlate well with 5–10 m ARGO upper layer temperatures suggesting that the AMSR-E microwave SST patterns are suitable for the study of physical processes affecting the temperatures of the near-surface layer.

[29] A comparison with a time series of temperatures collected at 97 m depth from a mooring in the central Labrador Sea clearly shows how the AMSR-E microwave SSTs have the same magnitudes as the deeper temperatures in late fall through early spring. This homogeneity in the temperature of the upper layer suggests the type of vertical mixing events known to occur in this geographic region. The deep mixed layers are replaced in the summer when surface heating forms a significantly warmer surface layer with higher surface temperatures as revealed by the AMSR-E microwave SST time series. During the summer the microwave SST warms up departing from the deeper temperature time series.

[30] A comparison with a time series collected at 73 m depth from a mooring in the deep Labrador Current shows that the SST is either larger (during summer) or smaller (during the rest of the year) suggesting a stratified near surface layer in the boundary current throughout the year. The AMSR-E microwave SST series peaks about 3 months before the subsurface temperature series.

[31] The microwave SST fields make it possible for the first time to evaluate high-resolution numerical models through their simulated sea surface temperature patterns. The distribution of SSTs during winter may give information about the region where Labrador Seawater transformation may occur. While there is a general agreement between model and microwave SSTs, there are some interesting differences. In particular the intrusions of warm waters from the southeast and of cold waters from the Northeast into the central Labrador Sea are different in strength and position as can be seen in the model and microwave SST fields. Both intrusions are important in confining the region of deep mixed layer depths during winter (Chanut et al., submitted manuscript, 2006).

[32] During March the intrusion of warm waters from the Southeast reaches farther north in the model than in the mean microwave SST (Figure 12). In the model, the northward intrusion of warm waters is associated with a recirculation cell that seems to be overestimated by the model. However, microwave SSTs show year-to-year variability in the position of the boundary between cold SSTs in the central Labrador Sea and warmer SSTs south of it (Figure 10) suggesting a corresponding year-to-year variability in the strength of the recirculation cell.

[33] The intrusion of cold waters from the West Greenland Current into the central Labrador Sea along the migration pathway of the West Greenland Current eddies is stronger in the model than in the microwave SSTs. The main reason could be the simulated water mass characteristics in the shallow West Greenland Current, i.e., here the simulated surface waters are too cold. However, microwave SSTs show a band of warmer SSTs north of the main convection region that seems to be generated by the mixing of warmer and saltier subsurface water masses toward the surface. These warmer temperatures are underestimated in the present model simulations. The year-to-year variability in the band of warmer SSTs that can be seen in the microwave data (Figure 10) may have various causes. Among them are the interannual variability in the heat fluxes, in the strength of the West Greenland Current eddy generation or in the water mass characteristics in the West Greenland Current.

[34] Comparisons between mean monthly AMSR-E microwave SSTs and mean monthly SSTs of high spatial resolution numerical model reveal general consistency. While the higher spatial resolution of the model depicts individual features of the circulation by their SST patterns like eddies and small intrusions, there are also features in the AMSR-E microwave SST patterns that do not occur in the model SSTs.

[35] **Acknowledgments.** This work was supported by the German Science Foundation (DFG) as part of the "Sonderforschungsbereich" SFB 460 "Dynamics of Thermohaline Circulation Variability". W. Emery's visit to IFM-GEOMAR was also supported by this same SFB. W. Emery's summer salary was paid by NASA Earth Science Enterprise, Physical Oceanography program (Eric Lindstrom program manager). The AMSR-E data were provided through the Web site of Remote Sensing Systems (RSS), and the infrared pathfinder data were acquired from the Physical Oceanography DAAC at NASA's Jet Propulsion Laboratory. AMSR-E data are produced by Remote Sensing Systems and sponsored by the NASA Earth Science REASON DISCOVER Project and the AMSR-E Science

Team. The ARGO data were collected and made freely available by the International Argo Project and the national programs that contribute to it. http://www.argo.ucsd.edu and http://argo.jcommops.org). Argo is a pilot program of the Global Ocean Observing System.

References

Brandt, P., F. Schott, A. Funk, and C. S. Martins (2004), Seasonal to interannual variability of the eddy field in the Labrador Sea from satellite altimetry, *J. Geophys. Res.*, *109*, C02028, doi:10.1029/2002JC001551.

Brandt, P., A. Funk, L. Czeschel, C. Eden, and C. Böning (2006), Ventilation and transformation of Labrador Sea Water and its rapid export in the deep Labrador Current, *J. Phys. Oceanogr*, in press.

Cuny, J., P. B. Rhines, P. P. Niiler, and S. Bacon (2002), Labrador Sea boundary currents and the fate of the Irminger Sea Water, *J. Phys. Oceanogr.*, *32*, 627–647.

Czeschel, L. (2004), The role of eddies for the deep water formation in the Labrador Sea, Ph.D. thesis, 95 pp., Univ. of Kiel, Kiel, Germany.

Eden, C., and C. Böning (2002), Sources of eddy kinetic energy in the Labrador Sea, *J. Phys. Oceanogr.*, *32*, 3346–3363.

Lavender, K. L., R. E. Davis, and W. B. Owens (2000), Mid-depth recirculation observed in the interior Labrador and Irminger Seas by direct velocity measurements, *Nature*, *407*, 66–69.

Lazier, J., R. Hendry, A. Clarke, I. Yashayaev, and P. Rhines (2002), Convection and restratification in the Labrador Sea, 1990–2000, *Deep Sea Res., Part I*, *49*, 1819–1835.

Lilly, J. M., P. B. Rhines, F. Schott, K. Lavender, J. Lazier, U. Send, and E. d'Asaro (2003), Observations of the Labrador Sea eddy field, *Prog. Oceanogr.*, *59*, 75–176.

Marshall, J., and F. Schott (1999), Open-ocean convection: Observations, theory, and models, *Rev. Geophys.*, *37*, 1–64.

Prater, M. D. (2002), Eddies in the Labrador Sea as observed by profiling RAFOS floats and remote sensing, *J. Phys. Oceanogr.*, *32*, 411–415.

Stramma, L., D. Kieke, M. Rhein, F. Schott, I. Yashayaev, and K. P. Koltermann (2004), Deep water changes at the western boundary of the subpolar North Atlantic during 1996 to 2001, *Deep Sea. Res., Part I*, *51*, 1033–1056.

C. Böning, P. Brandt, and A. Funk, IFM-GEOMAR, Duesternbrooker Weg 20, D-24105 Kiel, Germany.

W. J. Emery, Department of Aerospace Engineering Sciences, University of Colorado, Campus Box 431, Boulder, CO 80309, USA. (william.emery@colorado.edu)